HAL open science

Three-dimensional assessment of cardiac motion and deformation

Nicolas Duchateau, Filip Loncaric, Marta Sitges, Bart Bijnens

To cite this version:

Nicolas Duchateau, Filip Loncaric, Marta Sitges, Bart Bijnens. Three-dimensional assessment of cardiac motion and deformation. 3D echocardiography, 3rd edition, 2020. hal-02460177

HAL Id: hal-02460177

https://hal.science/hal-02460177v1

Submitted on 29 Jan 2020

HAL is a multi-disciplinary open access archive for the deposit and dissemination of scientific research documents, whether they are published or not. The documents may come from teaching and research institutions in France or abroad, or from public or private research centers.

L'archive ouverte pluridisciplinaire **HAL**, est destinée au dépôt et à la diffusion de documents scientifiques de niveau recherche, publiés ou non, émanant des établissements d'enseignement et de recherche français ou étrangers, des laboratoires publics ou privés.

This is a pre-print version. The final document will be available at http://www.crcpress.com/

3D Echocardiography, Third Edition
Takahiro Shiota, Ed.

Three-dimensional Assessment of Cardiac Motion and Deformation

Nicolas Duchateau[a], Filip Loncaric[b,c,d], Marta Sitges[b,c,d], Bart Bijnens[e,f]

[a] CREATIS, CNRS UMR 5220, INSERM U1206, Université Lyon 1, France;

[b] Cardiovascular Institute, Hospital Clínic, Universitat de Barcelona, Spain;

[c] Institut d'Investigacions Biomèdiques August Pi i Sunyer (IDIBAPS), Barcelona, Spain;

[d] Centro de Investigación Biomédica en Red Enfermedades Cardiovasculares (CIBERCV), Instituto de Salud Carlos III, Madrid, Spain;

[e] Universitat Pompeu Fabra, Barcelona, Spain;

[f] ICREA, Barcelona, Spain.

Keywords: Ventricular function; Myocardial motion; Myocardial deformation; Strain imaging; 3D Speckle tracking.

Corresponding author:

Bart Bijnens.

Information and Communications Technologies Department, Universitat Pompeu Fabra. c/ Roc Boronat 138, E08018 Barcelona, Spain.

E-mail: bart.bijnens@upf.edu

1. Introduction

Echocardiography is an evolving modality whose recent improvements facilitate the assessment of 3D motion and deformation, from routine evaluation to research on finer aspects of the cardiac function.

First, image sequences contain local interference patterns (the speckles), which are consistent with the tissue mechanics across a few consecutive frames, and therefore can be tracked to estimate motion and deformation [1]. With 3D imaging, such patterns are accessible everywhere and provide higher consistency in the tracking, contrary to 2D imaging where speckles may jump out of the plane due to the 3D nature of cardiac motion. Besides, 3D assessment no longer requires approximating the 3D cardiac mechanics from 2D projections.

Then, its temporal resolution is relatively high for the assessment of cardiac mechanics: around 40-60 frames/s in 2D, and 20-50 frames/s in 3D. Such a resolution is necessary for the assessment of fast events, and more generally for the accuracy of measurements involving temporal derivatives (velocity and strain rate, from displacement and strain, respectively). Besides, a high enough temporal resolution guarantees the consistency of speckle patterns across frames, and therefore the accuracy of the estimated motion and deformation, with substantial inaccuracies observed below 20 frames/s [2].

Currently, the use of 3D no longer stands as a limitation [3] and is accompanied by promising perspectives to improve the temporal resolution to very high frame rates [4], and the automation of post-processing tasks such as segmentation [5].

The main challenges for the quantification of cardiac mechanics from 3D echocardiography consist from the technical side in stabilizing the quality of images and the post-processing techniques, and from the user perspective in properly apprehending 3D during the acquisition and the data interpretation.

This chapter therefore proposes an overview of the quantification of cardiac motion and deformation through 3D echocardiography, with special attention on cardiac mechanics to properly interpret and use this technique. This review complements other published reviews on motion and deformation estimation in echocardiography [6-9] and specifically insights on 3D [2,10,11], and the chapters in previous editions of this book [12,13].

2. Myocardial motion and deformation

Cardiac mechanics are by definition in 3D. Simplifying the ventricles to 3D semi ellipsoids is already of great help for approximating global parameters from 2D such as volumes, and understanding basic mechanisms of the cardiac chambers [9]. Looking more in detail at the cardiac structure, cardiac motion and deformation are governed by the 3D arrangement of the myofibers within the wall, with an angle of inclination that varies gradually between the epicardial, midmyocardial, and endocardial layers [14].

Three orthogonal directions are therefore locally defined over the ventricular meshes to better characterize the main components of cardiac mechanics in healthy and diseased cases: radial (from the endocardium to the epicardium), longitudinal (from the base to the apex), and circumferential (along the circumference). Deformation of a local piece of myocardial tissue is a combination of longitudinal and circumferential shortening, radial thickening, and shearing (Figure 1). The proportion of each component is mainly determined by the wall properties, such as tissue contractility but also its composition, elasticity, incompressibility, etc. In particular, incompressibility directly relates the components along the three local directions, where longitudinal and circumferential shortenings are coupled with radial thickening to preserve tissue volume.

Given these simple considerations, a good imaging technique and its associated postprocessing should be able to recover these components of wall motion and deformation, encoded by displacement and strain, respectively. Displacement is a 3D vector that corresponds to a difference in position between a given instant and the onset of the cycle. Strain encodes a difference in the elongation of a small piece of tissue also compared with the cycle onset. Figure 2 illustrates this concept in 1D (straight line) and 3D (surface or volume elements). It roughly corresponds to the spatial derivative of the displacement vector, which for 3D volumes is a 3D tensor (3 × 3 matrix). We often only quantify its diagonal coefficients, which correspond to the radial, circumferential, and longitudinal strain accessible in most commercial software. Positive and negative strain corresponds to stretching and shortening, respectively. The extra-diagonal coefficients encode shearing and may also have a substantial contribution to the 3D tissue deformation (Figure 3), as in the presence of rotation or twisting [15] between the basal and apical levels (also denoted torsion after normalization by the ventricular height [16]). The segmental/local changes should be considered, independently of global measurements (Figure 4): global contraction may be the same between two cases, despite reduced or exaggerated contraction locally, related to e.g. differences in the tissue viability.

Area strain was proposed to overcome inaccuracies in estimating the radial component of deformation [17], already marked for the left ventricle and unavoidable for the thin wall of the right ventricle. It represents the deformation of surface elements, and is often calculated as the product of longitudinal and circumferential strain components, which should correspond to the inverse of the radial strain component if the volume of local elements is preserved under deformation.

Finally, changes in motion and deformation at a given instant can be complemented by the estimation of velocity and strain rate, which correspond to the temporal derivatives of displacement and strain, respectively (Figure 5).

This is a pre-print version. The final document will be available at http://www.crcpress.com/

3. How to measure motion and deformation

Basic principles of tracking

Speckle tracking consists in following local image patches containing some speckles between consecutive frames. The algorithm first locates a given patch in the next frame using block matching or local image similarity comparisons. The displacement of this patch between two consecutive frames corresponds to an approximation of myocardial motion between these instants (Figure 6). Then, motion is estimated along the whole sequence by chaining the displacements obtained for each pair of consecutive frames.

In practice, tracking is performed for speckles within the myocardium (estimation of wall motion and deformation), and more recently within the cavity after specific image post-processing (estimation of intra-cavity flow) [18]. The technique therefore requires segmenting the cardiac wall at given instants (for 3D, generally end-diastole and end-systole). This segmentation defines the region of interest for tracking, and provides a first estimation of *global* motion to further constrain the tracking of speckles and the estimation of *local* deformation.

Although little information exists on the algorithms used in commercial software, most are based on published approaches [19-21]. Nonetheless, substantial efforts are required on the validation of this technique and on the training of clinical operators.

Alternative approaches

Image registration also allows estimating displacement by comparing pairs of frames along the sequence. Contrary to speckle tracking, this technique matches the full echocardiographic images and not only the matching of blocks defined locally. It can therefore operate on pairs of consecutive frames (which then requires chaining pairwise transformations to estimate the displacement from the onset of the cycle), or directly match a given frame to the one at end-diastole. A transformation model

(locally affine, spline, etc.) defines the amount of freedom in the estimated matching, and therefore the complexity of the estimated deformation. This technique is widely used in the academic community as visible in recent validation initiatives [22-24]. As it operates on full images and not only speckles, it is not specific to echocardiography and may be applied to any imaging modality.

Additional knowledge can be incorporated to the tracking. *Shape models* can guide the tracking and provide physiologically plausible segmentations along the sequences. Such models are generally obtained from a population of healthy and diseased subjects using statistical learning techniques. Although not explicitly reported in scientific publications, some vendors mention that such models are used in their tracking software in 2D [25] and 3D [26]. *Biomechanical constraints* can be used in the transformation model, such as temporal consistency [27], or incompressibility [28].

Tissue Doppler differs from the previous methods. It does not aim at matching image contents, but analyzes phase shifts of the returning echoes from which local motion and deformation can be calculated along the beam direction. It therefore has a much higher temporal resolution compared to speckle tracking (around 200 frames/s). However, it requires aligning the beam parallel/orthogonal to the wall, for the recovery of longitudinal (apical view) or radial (parasternal view) velocities. Manual tracking of the observation points is offered in some software to prevent inadequate measurements from the originally fixed observation point.

Standardization and validation

The tracking algorithms involve several processing steps and assumptions that should be standardized. Joint initiatives including the European Association of Cardiovascular Imaging, the American Society Echocardiography, and academic and

industrial actors are currently focusing on this issue for segmentation [29] and tracking [30].

Indeed, differences between manufacturers exist in the definition of the myocardial segments, the intrinsic definition of strain, which myocardial layer to process, the post-processing applied (e.g. spatial and temporal smoothing), etc. In particular, the computation of radial strain differs between vendors: some prefer its estimation from area strain (the product of longitudinal and circumferential components, upon elemental volume conservation assumptions) rather than its direct estimation from 3D images, for which the low spatial resolution across the wall thickness is an issue.

Several validation studies recently reported on the performance of academic and commercial software on standardized datasets, including realistic simulated images for which ground truth motion is known [22-24,31,32]. They revealed substantial differences in the output measurements. As a result the estimation of global longitudinal parameters is often emphasized to go beyond ejection fraction [33], while looking the circumferential and radial components, and more local pattern changes is still limited to research.

Recommendations for the use of 3D speckle tracking

Speckle tracking is intensity-based and therefore requires good *image quality* and optimal acquisition. Poor or exaggerated contrast in the walls, acoustic shadowing or reverberations, and out-of-window or dropout artifacts are some of the main imaging factors that can lower the tracking accuracy. Random noise, lower wall visibility, and fuzzier endocardial/epicardial delineations may be additional limitations for 3D tracking. The lateral/anterior wall and apical regions are particularly challenging to image in 3D (e.g., field-of-view in dilated hearts, or limited possibilities for optimizing the image quality in the clinical workflow). Besides, the spatiotemporal resolution of 3D images is still low compared with 2D images, with consequences on the tracking accuracy: low spatial resolution affects the quality of the speckle patterns and their

resolution, and low temporal resolution can distort measurements of fast events (e.g. during isovolumic contraction/relaxation or at high heart rates) and even normal patterns [2].

In practice, analyzing a whole dataset can take a non-negligible amount of time, around 10 minutes for 3D depending on how practical the software interface is. Understanding the *post-processing* chain is therefore key to reach more reliable measurements and be critical on the output values.

The user is often asked to correct end-diastolic and end-systolic contours, which serve to initialize the tracking of endocardial and epicardial contours along the sequence. The software often allows correction of the contours propagated along the whole sequence, before the local tracking of speckles: we highly recommend the user to carefully check and correct the contours over the whole cycle and navigating across the whole 3D images. After the tracking of speckles, namely once the motion and deformation output is available, the user may also enable/disable several corrections that can substantially affect the output. Spatial and temporal smoothing is often applied to reduce noise in the estimated curves, which may hide local spatial and temporal abnormalities depending on the studied disease. We generally recommend turning down this option when available. Finally, drift artifacts may arise from the accumulation of errors along the cycle. The transformation estimated between consecutive frames is only an approximation of the true displacement: this error is probably negligible between consecutive frames, but accumulating the transformations along the cycle to obtain displacements from end-diastole may substantially amplify these small errors. Most 2D commercial software propose a drift correction, which assumes that cardiac motion is cyclic and therefore constrain displacement and strain at the end of the cycle to match their values at the onset of the cycle (Figure 6). In 3D, this option may not be directly accessible to the user, but still can be implemented on homemade software from the exported outputs (Figures 7 to 10). Note that this correction does not concern myocardial velocity and strain

rate, which correspond to instantaneous parameters and are not affected by the accumulation of errors.

4. Practical examples

a. Healthy control (Figure 7*)

An active, healthy, 30-year-old male, with no significant medical history or cardiac disease. The echocardiographic 'window' is optimal. Left ventricle is of normal dimensions, and the ejection fraction is preserved (60%). 2D speckle-tracking deformation shows that global longitudinal function is in the normal range. The segmental deformation values are uniform, as well as the timings of strain curves. 4D deformation analysis shows a similar global longitudinal function, with uniform and synchronous segmental deformation.

b. Healthy athlete (Figure 8*)

A healthy, 42-year-old male athlete, training long-distance running six days a week for the last 6 years. The left ventricle is representative of early stage changes that are seen in athletes participating in endurance training associated with repetitive chronic volume overload. Over time, these alterations result in eccentric left ventricular hypertrophy with increased wall thickness and overall mass, coupled with comparably increased end-diastolic volumes and associated increase in stroke volume so that EF and global deformation at rest will be at the lower side. 2D speckle-tracking deformation shows that global longitudinal function is slightly decreased, which is in line with the enlarged athlete's heart and not related to intrinsic dysfunction. The segmental deformation values are uniform. 4D deformation analysis shows a similar global longitudinal function, with uniform segmental deformation.

c. Hypertension (Figure 9*)

A 57-year-old male patient with long-standing arterial hypertension on antihypertensive therapy and with preserved left ventricular ejection fraction (60%). The left ventricle shows signs of a generalized myocardial wall thickening indicative of hypertensive heart disease; however, left ventricular mass is still in the normal range. 2D speckle-tracking analysis shows that global longitudinal function is normal. Segmental deformation reveals a characteristic pattern of impaired basal septal deformation. In the setting of increased blood pressure, due to the increased local radius of curvature, the basal septal segment is the first to show systolic dysfunction, quantifiable by changes in deformation - decrease in longitudinal strain. 4D deformation analysis shows a slightly higher global longitudinal function, nevertheless, the characteristic pattern of basal septal impairment is still notable.

d. Hypertrophic cardiomyopathy (Figure 10*)

A 42-year-old male patient with diagnosed hypertrophic cardiomyopathy (HCM) and preserved ejection fraction (52%). Localized myocardial wall thickening can be recognized in the anterior and inferior septum, as well as in the inferior wall, resulting in elevated indexed left ventricular mass. The maximal thickness is seen at the inferior part of the septum measuring 22 mm. 2D speckle-tracking deformation analysis demonstrates characteristic findings in HCM - significant heterogeneity in regional myocardial deformation is paired with the noticeable heterogeneity in wall thickness. The greatest reduction in longitudinal strain is seen in the interventricular septum. Areas of abnormal deformation are surrounded by normal deformation in the same ventricular region, a finding conceivably related to the heterogeneous distribution of myocardial disarray. As compared to findings of basal septal impairment in arterial hypertension, the impairment seen in HCM is considerably more pronounced. Global longitudinal strain is only slightly reduced. 4D deformation analysis demonstrates a similar heterogenic pattern of myocardial deformation.

This is a pre-print version. The final document will be available at http://www.crcpress.com/

5. Conclusion

Speckle tracking is an essential tool for the assessment of cardiac mechanics, in particular through 3D motion and deformation. The technique is at the crossroad of developments on imaging itself (3D and high frame rate sequences), automation of the processing (segmentation and tracking), and validation/standardization initiatives. Substantial improvements are therefore expected in the near future. Nonetheless, using such tools will still require a cautious use in light of the technology behind, appropriate training on the acquisition, the use of processing software, and the interpretation of the results in light of the pathophysiology of the observed subjects.

Acknowledgements

Funding

This work was partially supported by the Spanish Ministry of Economy and Competitiveness [grant TIN2014-52923-R; Maria de Maeztu Units of Excellence Programme - MDM-2015-0502] and FEDER, and the European Union H2020 programme [PIC H2020-MSCA-ITN-2017-764738].

Conflict of interest

In the recent years, MS received speaker fees from GE Healthcare, Toshiba, Medtronic, and Abbott; BB received speaker fees from GE Healthcare. However, these did not influence the contents of this chapter, which was independently designed and did not involve any sponsorship.

This is a pre-print version. The final document will be available at http://www.crcpress.com/

References

(1) Garcia D, Lantelme P, Saloux E. Introduction to speckle tracking in cardiac ultrasound imaging. In: Loizou CP, Pattichis CS, D'hooge J, ed. *Handbook of speckle filtering and tracking in cardiovascular ultrasound imaging and video.* Institution of Engineering and Technology, 2018.

(2) Amzulescu MS, De Craene M, Langet H, et al. Myocardial strain imaging: review of general principles, validation, and sources of discrepancies. *Eur Heart J Cardiovasc Imaging*. 2019;20:605-19.

(3) Lang RM, Addetia K, Narang A, et al. 3-dimensional echocardiography: latest developments and future directions. *JACC Cardiovasc Imaging*. 2018;11:1854-78.

(4) Cikes M, Tong L, Sutherland GR, et al. Ultrafast cardiac ultrasound imaging: technical principles, applications, and clinical benefits. *JACC Cardiovasc Imaging*. 2014;7:812-23.

(5) Leclerc S, Smistad E, Pedrosa J, et al. Deep learning for segmentation using an open large-scale dataset in 2D echocardiography. *IEEE Trans Med Imaging*. 2019;38:2198-210.

(6) Bijnens BH, Cikes M, Claus P, et al. Velocity and deformation imaging for the assessment of myocardial dysfunction. *Eur J Echocardiogr.* 2009;10:216-26.

(7) Cikes M, Sutherland GR, Anderson LJ, et al. The role of echocardiographic deformation imaging in hypertrophic myopathies. *Nat Rev Cardiol.* 2010;7:384-96.

(8) Mor-Avi V, Lang RM, Badano LP, et al. Current and evolving echocardiographic techniques for the quantitative evaluation of cardiac mechanics. *J Am Soc Echocardiogr.* 2011;24:277-313.

(9) Bijnens B, Cikes M, Butakoff C, et al. Myocardial motion and deformation: What does it tell us and how does it relate to function? *Fetal Diagn Ther.* 2012;32:5-16.

(10) Cheung YF. The role of 3D wall motion tracking in heart failure. *Nat Rev Cardiol.* 2012;9:644-57.

(11) Jasaityte R, Heyde B, D'hooge J. Current state of three-dimensional myocardial strain estimation using echocardiography. *J Am Soc Echocardiogr.* 2013;26:15-28.

(12) Stoylen A. Strain echocardiography. In: Shiota T, ed. *3D Echocardiography.* London: Informa Healthcare, 2007:141-51.

(13) Duchateau N, Bijnens BH, D'hooge J, et al. Three-dimensional assessment of cardiac motion and deformation. In: Shiota T, ed. *3D echocardiography, 2nd edition*. CRC press, 2013;201-13.

(14) Vendelin M, Bovendeerd PH, Engelbrecht J, et al. Optimizing ventricular fibers: Uniform strain or stress, but not ATP consumption, leads to high efficiency. *Am J Physiol Heart Circ Physiol.* 2002;283:H1072-81.

(15) Ashraf M, Zhou Z, Nguyen T, et al. Apex to base left ven- tricular twist mechanics computed from high frame rate two-dimensional and three-dimensional echocardiography: A comparison study. *J Am Soc Echocardiogr.* 2012;25:121-28.

(16) Henson RE, Song SK, Pastorek JS, et al. Left ventricular torsion is equal in mice and humans. *Am J Physiol Heart Circ Physiol.* 2000;278:H1117-23.

(17) Seo Y, Ishizu T, Enomoto Y, et al. Endocardial surface area tracking for assessment of regional LV wall deformation with 3D speckle tracking imaging. *JACC Cardiovasc Imaging.* 2011;4:358-65.

(18) Assi KC, Gay E, Chnafa C, Mendez S, Nicoud F, Abascal JFPJ, Lantelme P, Tournoux F, Garcia D. Intraventricular vector flow mapping-a Doppler-based

regularized problem with automatic model selection. *Phys Med Biol*. 2017;62:7131-47.

(19) Adam D, Landesberg A, Konyukhov E, et al. On changing coordinate systems for longitudinal tensor-based morphometry. *Proceedings IEEE Computers in Cardiology.* 2004:337-40.

(20) Behar V, Adam D, Lysyansky P, et al. The combined effect of non-linear filtration and window size on the accuracy of tissue displacement estimation using detected echo signals. *Ultrasound.* 2004; 41:743-53.

(21) Leitman M, Lysyansky P, Sidenko S, et al. Two-dimensional strain - a novel software for real-time quantitative echocardiographic assessment of myocardial function. *J Am Soc Echocardiogr.* 2004;17:1021-9.

(22) Tobon-Gomez C, De Craene M, McLeod K, et al. Benchmarking framework for myocardial tracking and deformation algorithms: An open access database. *Med Image Anal*. 2013;17:632-48.

(23) De Craene M, Marchesseau S, Heyde B, et al. 3D strain assessment in ultrasound (Straus): a synthetic comparison of five tracking methodologies. *IEEE Trans Med Imaging.* 2013;32:1632-46.

(24) Alessandrini M, Heyde B, Queiros S, et al. Detailed evaluation of five 3D speckle tracking algorithms using synthetic echocardiographic recordings. *IEEE Trans Med Imaging.* 2016;35:1915-26.

(25) Knight DS, Schwaiger JP, Krupickova S, Davar J, Muthurangu V, Coghlan JG. Accuracy and test-retest reproducibility of two-dimensional knowledge-based volumetric reconstruction of the right ventricle in pulmonary hypertension. *J Am Soc Echocardiogr*. 2015;28:989-98.

(26) Schreckenberg M, inventor; Tomtec Imaging Systems GmbH, assignee. Adaptation of a 3D-surface model to boundaries of an anatomical structure in a 3D-image data set. *United States patent* US9280816B2, 2013.

(27) De Craene M, Piella G, Camara O, et al. Temporal diffeomorphic free-form deformation: application to motion and strain estimation from 3D echocardiography. *Med Image Anal*. 2012;16:427-50.

(28) Mansi T, Pennec X, Sermesant M, et al. iLogDemons: a demons-based registration algorithm for tracking incompressible elastic biological tissues. *Int J Comput Vis*. 2011;92:92-111.

(29) Papachristidis A, Galli E, Geleijnse ML, et al. Standardized delineation of endocardial boundaries in three-dimensional left ventricular echocardiograms. *J Am Soc Echocardiogr.* 2017;30:1059-69.

(30) Voigt JU, Pedrizzetti G, Lysyansky P, et al. Definitions for a common standard for 2D speckle tracking echocardiography: consensus document of the EACVI/ASE/Industry Task Force to standardize deformation imaging. *Eur Heart J Cardiovasc Imaging.* 2015;16:1-11.

(31) D'hooge J, Barbosa D, Gao H, et al. Two-dimensional speckle tracking echocardiography: standardization efforts based on synthetic ultrasound data. *Eur Heart J Cardiovasc Imaging.* 2016;17:693-701.

(32) Alessandrini M, Chakraborty B, Heyde B, Bernard O, De Craene M, Sermesant M, D'Hooge J. Realistic vendor-specific synthetic ultrasound data for quality assurance of 2-D speckle tracking echocardiography: simulation pipeline and open access database. *IEEE Trans Ultrason Ferroelectr Freq Control*. 2018;65:411-22.

(33) Cikes M, Solomon SD. Beyond ejection fraction: an integrative approach for assessment of cardiac structure and function in heart failure. *Eur Heart J.* 2016;37:1642-50.

Figure legends

Figure 1: The three anatomical directions of myocardial motion and deformation. (a-b-c) Progressive zoom on a portion of the myocardium with the radial, circumferential, and longitudinal directions overlaid. (d) Expected changes for this portion during systole, for a healthy myocardium.

Figure 2: Illustration of the values quantified in strain in 1D (a) and 3D (b-c). In case of surface meshes, as in current 3D right ventricular applications, the concept of area strain extends the 1D definition to local area changes. In case of volume meshes, strain is a 3x3 matrix whose diagonal coefficients correspond to forces orthogonal to the elemental surface, while non-diagonal coefficients relate to forces parallel to the elemental surface (shearing).

Figure 3: Illustration of local variations in all the strain components (infinitesimal strain definition) for a 2D material that undergoes pure shear (a) or a more complex deformation with both shearing and stretching along the horizontal axis (b).

Figure 4: Importance of the quantification of global and local deformation: two walls shortening equally overall (75% of their initial length), but with a very different local behavior due to different tissue viability.

Figure 5: Longitudinal displacement, velocity, strain, and strain rate for a healthy volunteer at different levels of the septum, obtained by 2D speckle tracking. Vertical bars indicate specific events of the cardiac cycle: onset of QRS (Q1 and Q2), and mitral/aortic opening/closure (MVO/MVC and AVO/AVC).

Figure 6: Conservation of speckles over consecutive frames, allowing tracking along the cycle (a). Illustration of the link between displacement and instantaneous velocities (b). The accumulation of small errors along the sequence may require compensating for drifting (c).

Figure 7*: 4D deformation analysis for a healthy subject. Longitudinal, circumferential, area, and radial strain traces and end-systolic patterns, after drift correction. 3D echocardiographic sequence provided as video.

Figure 8*: 4D deformation analysis for a healthy athlete. Display similar to Figure 7*.

Figure 9*: 4D deformation analysis for a hypertensive patient. Display similar to Figure 7*.

Figure 10*: 4D deformation analysis for a patient with hypertrophic cardiomyopathy. Display similar to Figure 7*.

This is a pre-print version. The final document will be available at http://www.crcpress.com/

Figure 1

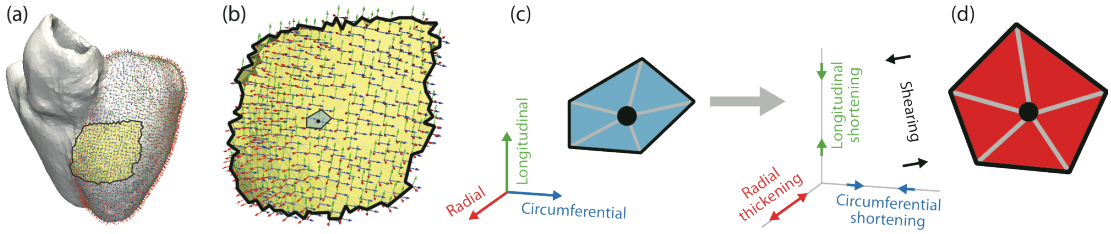

This is a pre-print version. The final document will be available at http://www.crcpress.com/

Figure 2

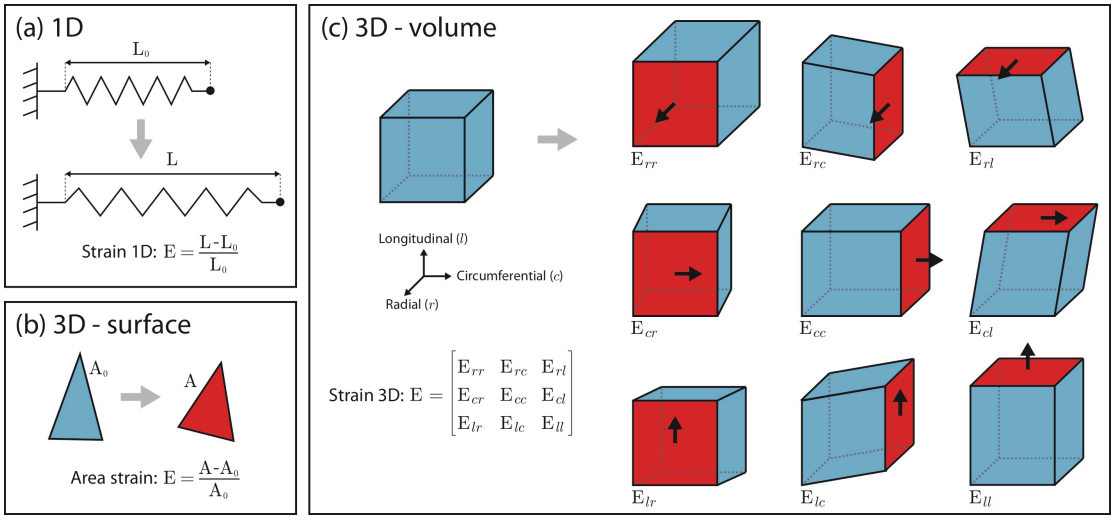

This is a pre-print version. The final document will be available at http://www.crcpress.com/

Figure 3

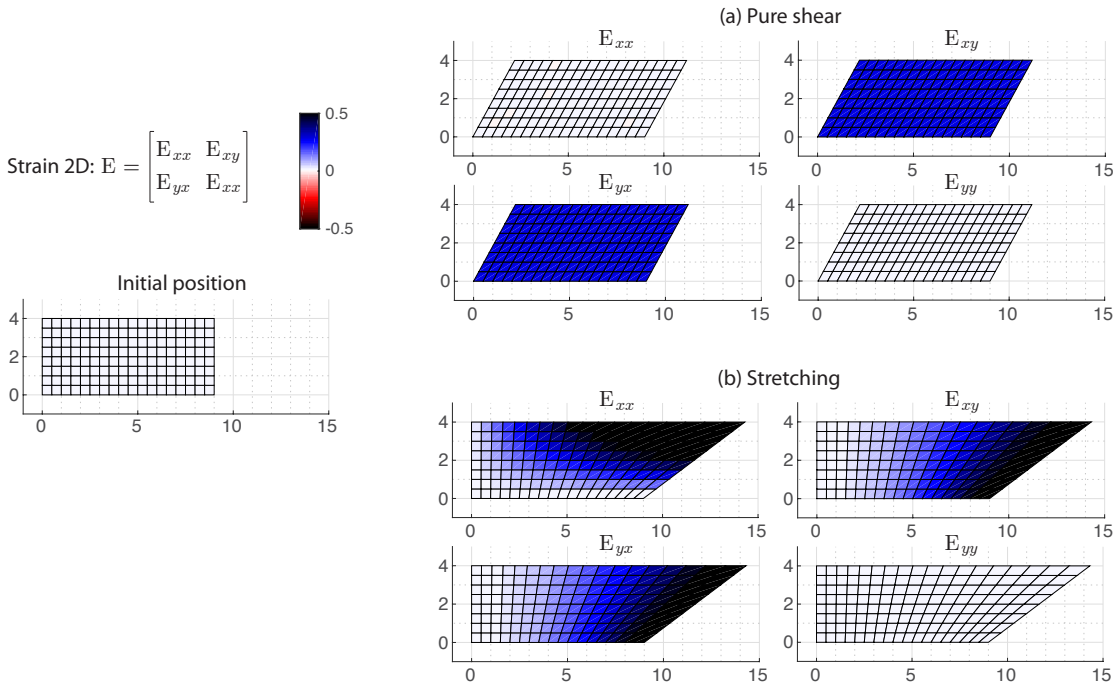

This is a pre-print version. The final document will be available at http://www.crcpress.com/

Figure 4

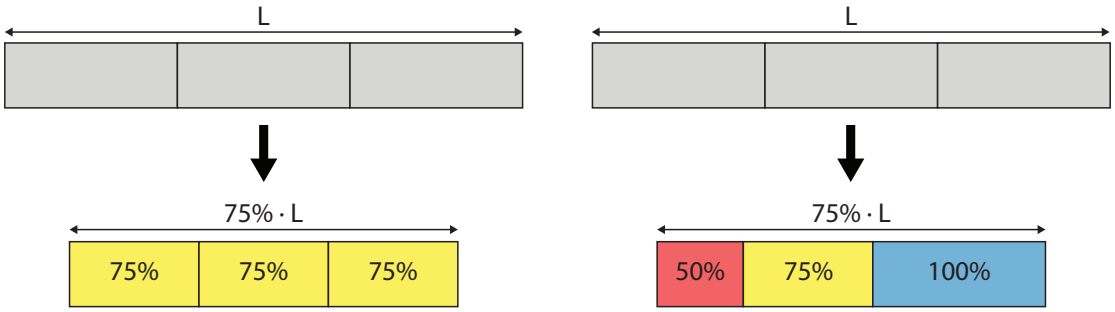

This is a pre-print version. The final document will be available at http://www.crcpress.com/

Figure 5

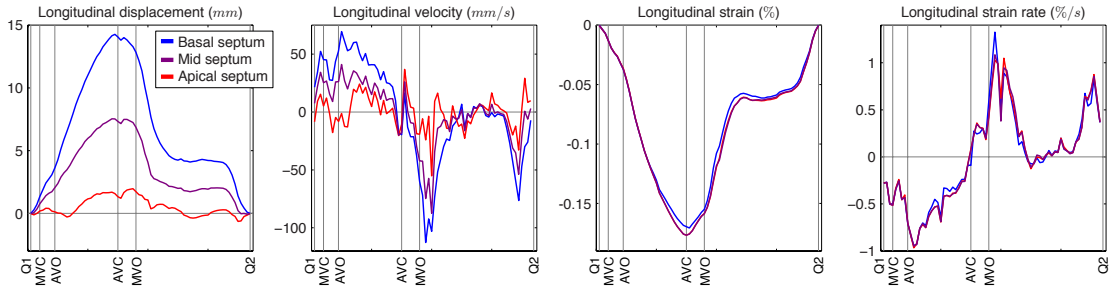

This is a pre-print version. The final document will be available at http://www.crcpress.com/

Figure 6

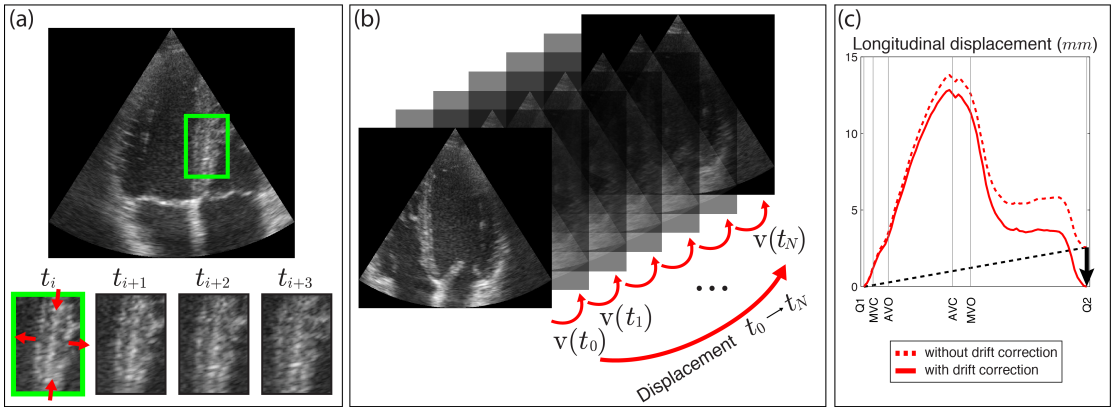

This is a pre-print version. The final document will be available at http://www.crcpress.com/

Figure 7

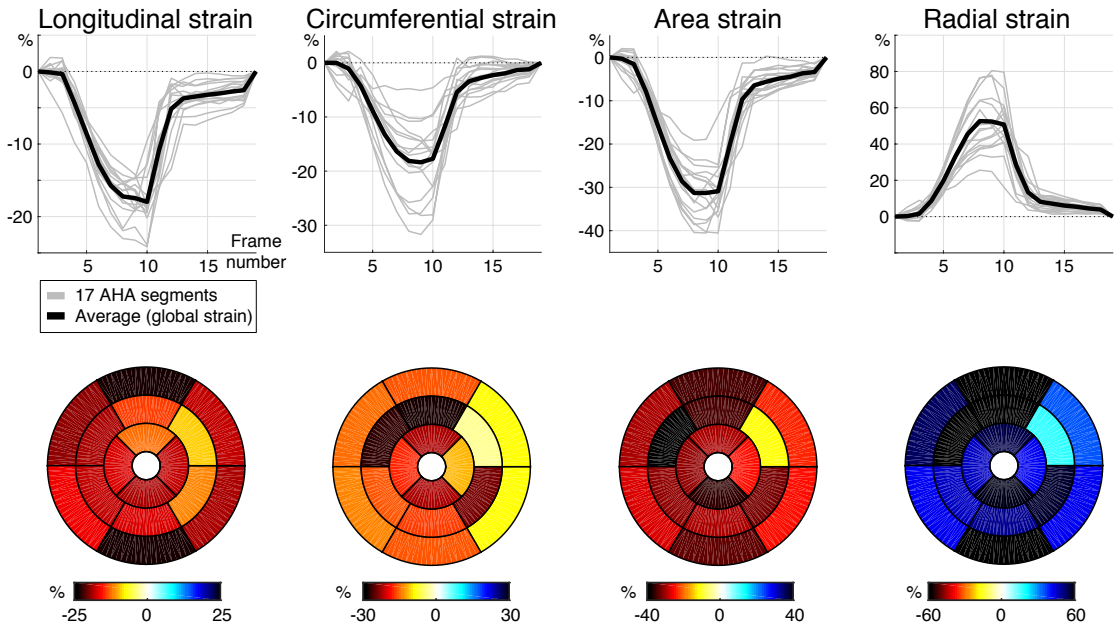

This is a pre-print version. The final document will be available at http://www.crcpress.com/

Figure 8

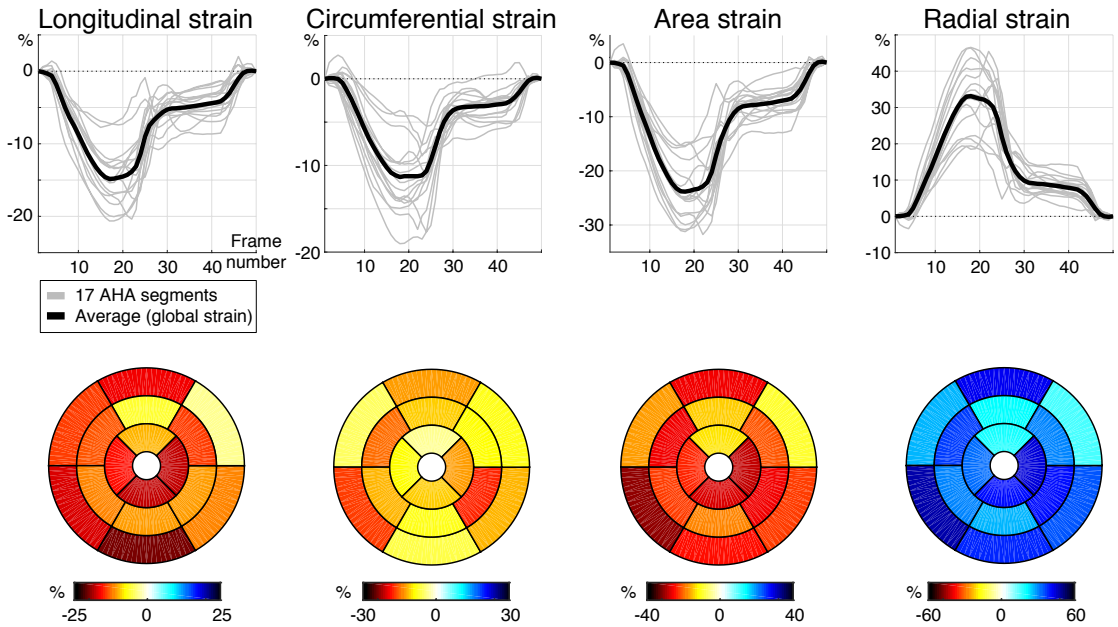

This is a pre-print version. The final document will be available at http://www.crcpress.com/

Figure 9

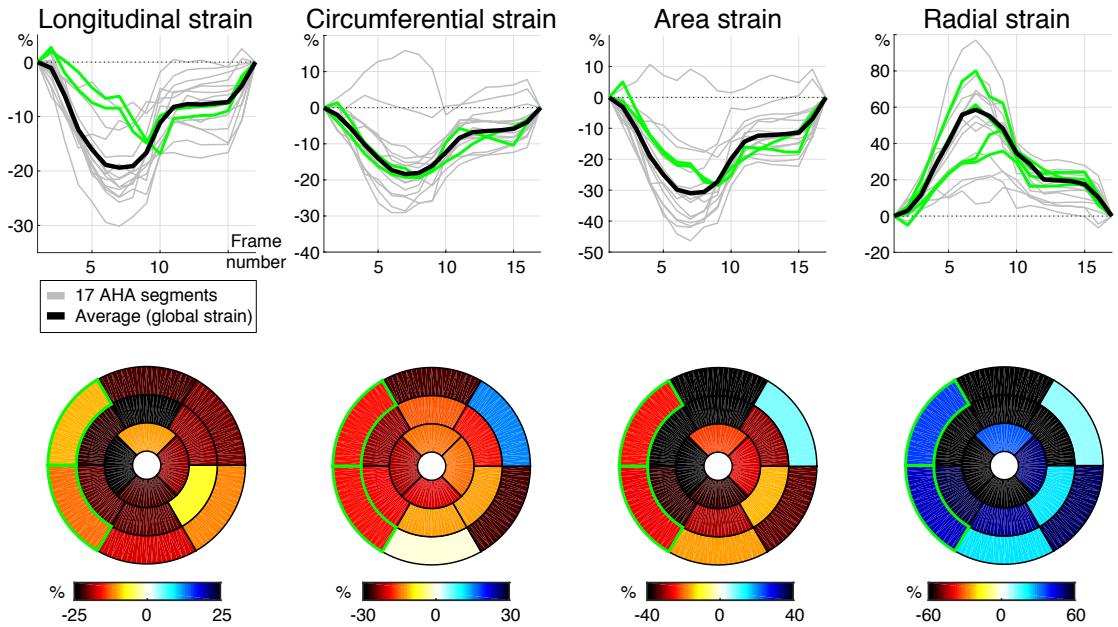

This is a pre-print version. The final document will be available at http://www.crcpress.com/
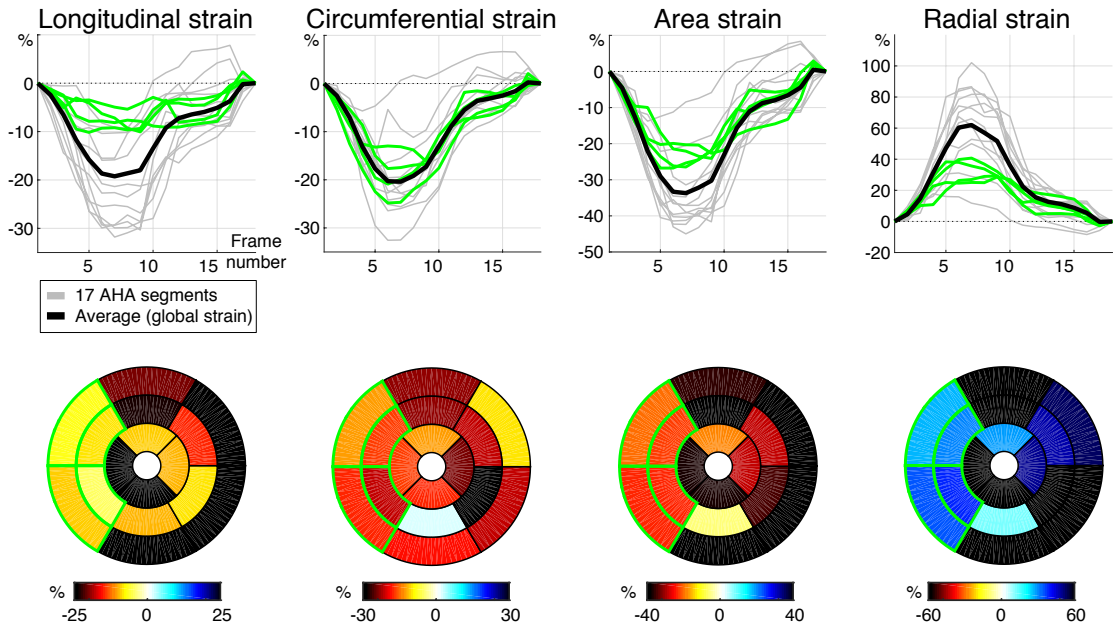
Figure 10